sustainability

MDPI

Article

The Impact of Seasonal Climate on Dryland Vegetation NPP: The Mediating Role of Phenology

Xian Liu [1], Hengkai Li [1,*], Yanbing Zhou [2,*], Yang Yu [1] and Xiuli Wang [3]

[1] School of Civil and Surveying & Mapping Engineering, Jiangxi University of Science and Technology, Ganzhou 341000, China; 6120220131@mail.jxust.edu.cn (X.L.); 1220211013@mail.jxust.edu.cn (Y.Y.)
[2] Information Technology Research Center, Beijing Academy of Agriculture and Forestry Sciences, Beijing 100097, China
[3] School of Economics and Management, Jiangxi University of Science and Technology, Ganzhou 341000, China; 9120040029@jxust.edu.cn
* Correspondence: giskai@jxust.edu.cn (H.L.); zhouyb@nercita.org.cn (Y.Z.)

Abstract: Dryland ecosystems are highly sensitive to climate change, making vegetation monitoring crucial for understanding ecological dynamics in these regions. In recent years, climate change, combined with large-scale ecological restoration efforts, has led significant greening in China's arid areas. However, the mechanisms through which seasonal climate variations regulate vegetation growth are not yet fully understood. This study hypothesizes that seasonal climate change affects net primary productivity (NPP) of vegetation by influencing phenology. We focused on China's Windbreak and Sand-Fixation Ecological Function Conservation Areas (WSEFCAs) as representative regions of dryland vegetation. The Carnegie–Ames–Stanford Approach (CASA) model was used to estimate vegetation NPP from 2000 to 2020. To extract phenological information, NDVI data were processed using Savitzky–Golay (S–G) filtering and threshold methods to determine the start of season (SOS) and end of season (EOS). The structural equation model (SEM) was constructed to quantitatively assess the contributions of climate change (temperature and precipitation) and phenology to variations in vegetation NPP, identifying the pathways of influence. The results indicate that the average annual NPP in WSEFCAs increased from 55.55 gC/(m^2·a) to 75.01 gC/(m^2·a), exhibiting uneven spatial distribution. The pathways through which seasonal climate affects vegetation NPP are more complex and uneven. Summer precipitation directly promoted NPP growth (direct effect = 0.243, $p < 0.001$) while also indirectly enhancing NPP by significantly advancing SOS (0.433, $p < 0.001$) and delaying EOS (−0.271, $p < 0.001$), with an indirect effect of 0.133. This finding highlights the critical role of phenology in vegetation growth, particularly in regions with substantial seasonal climate fluctuations. Although the overall ecological environment of WSEFCAs has improved, significant regional disparities remain, especially in northwestern China. This study introduces causal mediation analysis to systematically explore the mechanisms through which seasonal climate change impacts vegetation NPP in WSEFCAs, providing new insights into the broader implications of climate change and offering scientific support for ecological restoration and management strategies in arid regions.

Keywords: arid regions; causal mediation analysis; climate change; vegetation phenology; vegetation net primary productivity

Citation: Liu, X.; Li, H.; Zhou, Y.; Yu, Y.; Wang, X. The Impact of Seasonal Climate on Dryland Vegetation NPP: The Mediating Role of Phenology. *Sustainability* **2024**, *16*, 9835. https://doi.org/10.3390/su16229835

Academic Editors: Mou Leong Tan, Cheng Li, Fei Zhang and Kwok Pan Chun

Received: 4 October 2024
Revised: 1 November 2024
Accepted: 4 November 2024
Published: 11 November 2024

1. Introduction

Net primary productivity (NPP) refers to the net accumulation of organic matter by vegetation through photosynthesis over a given period. It is a key metric for measuring the carbon sources and sinks of ecosystems and plays a significant role in the study of the global carbon cycle [1,2]. Arid–semi-arid ecosystems have been shown to exert a significant influence on the trend and interannual variability of the global terrestrial carbon sink over the past three decades [3]. These regions are particularly sensitive to climate change

and are often considered "outposts" of global change [4,5]. Changes in NPP in arid and semi-arid regions not only reflect the health of these ecosystems, but also exert a profound influence on the global carbon cycle [6]. Consequently, the monitoring and assessment of ecosystems in arid and semi-arid zones using indicators such as NPP represents a crucial step in understanding the ecological dynamics of these vulnerable regions. Furthermore, it provides invaluable data to support for the response to global climate change and the sustainable development of ecosystems.

Vegetation phenology, as the response time of vegetation to seasonal changes, is among the most sensitive ecological indicators of climate change [7,8]. In arid–semi-arid regions, the extreme and fluctuating climatic conditions result in a more pronounced response of phenology to environmental changes [9]. The dynamics of vegetation phenology in these regions exert a direct influence on the seasonal fluctuations of NPP. In recent years, researchers have identified that warmer temperatures and altered precipitation patterns in arid regions may result in the advancement or postponement of climatic events [10,11], which in turn amplifies or weakens the seasonal dynamics of NPP. Such dynamic changes influence the carbon balance and ecosystem stability [12,13]. Consequently, a comprehensive investigation of vegetation phenology dynamics and its response to climate change in the arid zone constitutes a crucial foundation for understanding ecosystem functions in the arid zone.

In addressing environmental challenges such as desertification and soil degradation, China has established Windbreak and Sand-Fixation Ecological Function Conservation Areas (WSEFCAs) and initiated a series of ecological restoration initiatives in arid and semi-arid regions. Among these, the Three North Shelter Forest Project (TNSFP, 1979–2050) stands out as a prominent example [14,15]. WSEFCAs have played a key role in preventing wind and sand encroachment and safeguarding the ecological environment [16]. However, these regions experience significant seasonal climate changes, with high temperatures and droughts in the summer being particularly impactful on vegetation growth. These changes not only affect the growth cycle of vegetation but also lead to significant fluctuations in phenological events [17,18]. Drought has been shown to impair vegetation productivity [19], whereas climate warming may prolong growing seasons, thereby increasing crop yields in certain instances [20].

However, the effects of seasonal climate change on vegetation NPP are particularly complex, exhibiting substantial spatial variability and inconsistency [21]. In particular, the role that vegetation phenology plays in this phenomenon has not been widely explored [22]. To gain a deeper understanding of the complex mechanisms by which seasonal climate change affects dryland vegetation NPP, this study employed structural equation modeling (SEM). As a quantitative research method [23], SEM is capable of being widely utilized to explore direct and indirect relationships between multiple factors by establishing links between empirical data and theoretical analysis [24,25]. For example, Chen et al. [26] employed SEM to examine the multifaceted impacts of climate change and human activities on vegetation cover alterations in northern China. Similarly, Liu et al. [27] utilized SEM to ascertain the moderating influence of hydrothermal conditions on Normalized Difference Vegetation Index (NDVI) responses. These studies have demonstrated the unique advantages of SEM in revealing multifactor interactions in ecosystems. Accordingly, the present study employs SEM models for mediating effect analysis, thereby facilitating a comprehensive investigation of the complex factors and interactions that influence vegetation growth.

The present study sought to examine the intricate interrelationship between NPP and climatic variables, as well as the associated phenological shifts, in arid and semi-arid regions of China that are particularly vulnerable to ecological disruption. It hypothesized that the quantitative contributions of climate and phenological changes to vegetation growth and their impact pathways vary significantly across seasons. To validate this hypothesis, the principal objectives of this study are as follows: (1) reveal the spatial and temporal dynamics of vegetation NPP in China's arid protected areas during the period 2000–2020 and the contrasting differences in different regions; (2) identify the regularity of vegetation phenology under

different climatic and topographic conditions; (3) quantitatively analyze the mechanisms of the contribution of climatic factors and changes in vegetation phenology to NPP and their pathways of influence, especially to explore the regulatory mechanism of phenological changes on NPP under seasonal climate changes. The findings of this study contribute to our understanding of the dynamic processes by which dryland ecosystems respond to climate change. They also provide a scientific basis for the development of strategies for the conservation of these ecosystems and for the sustainable management of arid zones.

2. Materials and Methods

2.1. Study Area

The WSEFCA is situated in the arid and semi-arid zones of northern China (Figure 1), covering a total area of 374,000 square kilometers. The study area covers geographic regions, from the Tarim River Basin in the Xinjiang Uygur Autonomous Region to the Horqin and Maowusu Sandy lands in the Inner Mongolia Autonomous Region, featuring varied topographies. This area is a desertification-sensitive and fragile zone under continental climate conditions in China. The annual average temperature ranges from approximately 4 °C to 8 °C, and the annual precipitation increases gradually from 150 mm in the western part of the region to 250 mm in the eastern part [28]. These climatic conditions pose significant challenges for vegetation growth. At the beginning of this century, China launched a series of sand-prevention and -control programs aimed at effectively combating land desertification and wind erosion. These programs were designed to effectively address the threats of land desertification and wind erosion. The implementation of these programs has contributed to improved vegetation cover and mitigated the process of land desertification to some extent.

2.2. Data Sources

In this study, the years 2000, 2005, 2010, 2015 and 2020 were selected as the study time points with the aim of comprehensively analyzing the characteristics and influence mechanisms of vegetation NPP changes in the vegetation of the WSEFCA under climate change within this period.

The NDVI is derived from the MODIS MOD13A3 product of the National Aeronautics and Space Administration (NASA), with a spatial resolution of 1 km × 1 km and a temporal resolution of 30 days. The MODIS data are widely applicable in the study of global and regional vegetation changes, ecological monitoring and the response to natural disasters and extreme climatic events, among other areas of research. The MODIS data were employed to estimate vegetation NPP in the WSEFCA, thereby furnishing pivotal information for an in-depth understanding of the research topic (Table 1).

Table 1. Sources of data.

Data	Description	Resolution	Period	Source
Vegetation type	National 1:1,000,000 vegetation type map	Raster/1 km		China National Data Center for Glaciology and Geocryology, accessed on 10 November 2022. (http://www.ncdc.ac.cn)
NDVI	MOD13A3	Raster/1 km		NASA, accessed on 14 May 2023. (https://ladsweb.modaps.eosdis.nasa.gov/)
DEM	SETMDEMUTM	Raster/90 m	2000	Geospatial data cloud, accessed on 3 July 2023. (https://www.gscloud.cn)
	ASTER_GDEM_30M	Raster/30 m	2009	
	GDEMV2	Raster/30 m	2015	
	GDEMV3	Raster/30 m	2019	
Meteorological data	Precipitation and temperature	Gridded/0.5°	2000–2020	CRU TS v. 4.07, accessed on 15 November 2022. (https://crudata.uea.ac.uk/cru/data/hrg/)
	Solar radiation	Gridded/0.1°	2000–2020	ERA5-Land monthly averaged data from 1981 to present, accessed on 15 November 2022. (https://cds.climate.copernicus.eu)
Phenological data	Start of Season	Point	2001–2016	Vegetation phenology data set from major ecological observation stations in China, accessed on 27 July 2023. (https://doi.org/10.11922/sciencedb.449)

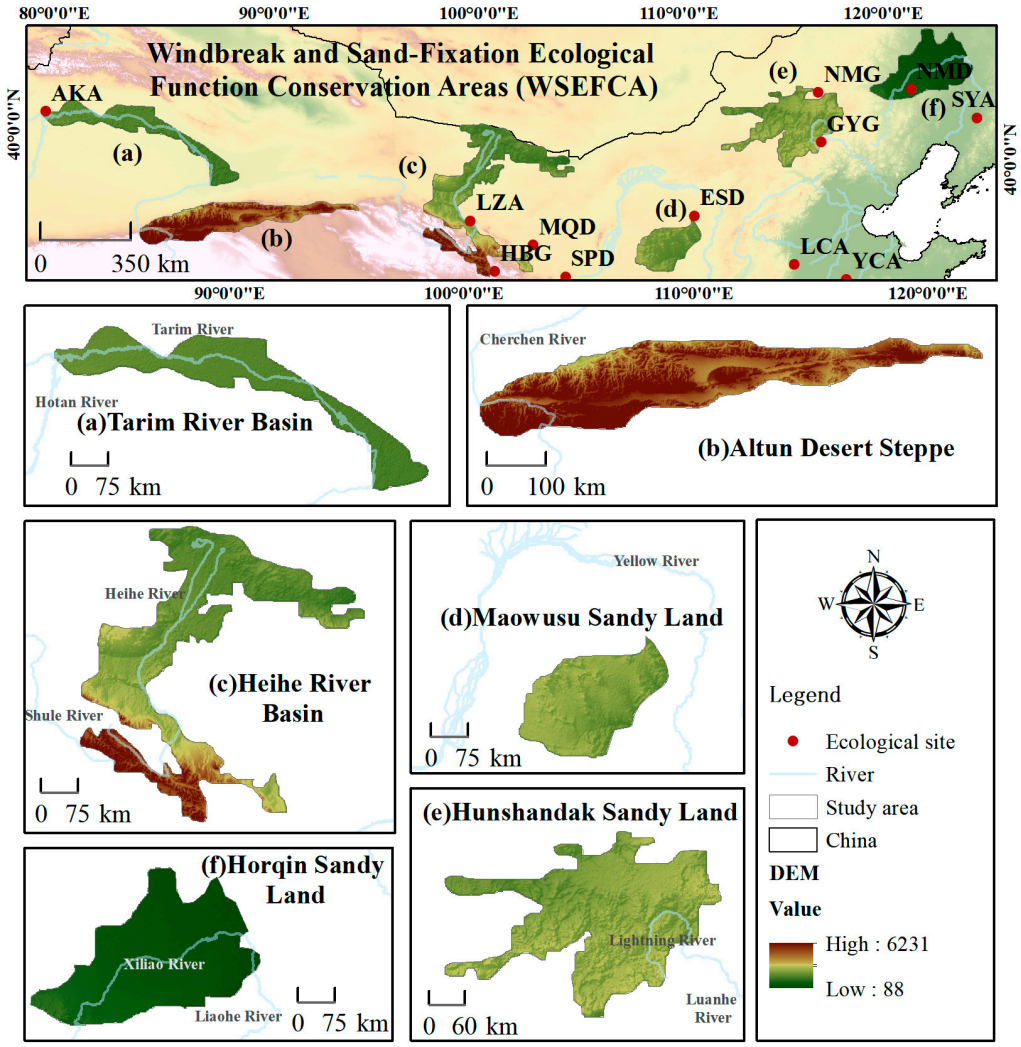

Figure 1. Study area. (**a**) Tarim River Basin (Tarim); (**b**) Altun Desert Steppe (Altun); (**c**) Heihe River Basin (Heihe); (**d**) Maowusu Sandland (Maowusu); (**e**) Hunshandak Sandland (Hunshandak); (**f**) Horqin Sandland (Horqin). Field observation stations: Aksu (AKA); Linze (LZA); Haibei (HBG); Minle (MQD); Shapotou (SPD); Ordos (ESD); Luancheng (LCA); Yucheng (YCA); Guyuan (GYG); Inner Mongolia (NMG); Naiman (NMD); Shenyang (SYA).

The temperature and precipitation data came from the CRU TS dataset of the UK National Center for Atmospheric Science (NCAS), with a spatial and temporal resolution of 0.5° per month. This dataset is one of the most widely utilized climate datasets currently available [29]. The radiometric data were derived from the ERA5-Land reanalysis product, which was provided by the European Center for Medium-Range Weather Forecasts (ECMWF), with a spatial and temporal resolution of 0.1°/month. The data have been demonstrated to have significant utility in arid and semi-arid regions [30].

The phenology validation data were selected from the vegetation climate dataset of major ecological observatories in China [31]. The dynamic thresholds for SOS and EOS of vegetation were validated using the 2015 phenology observation data from 12 stations, including Aksu, Ansai, Cele, Ordos, Haibei and Inner Mongolia.

The digital elevation model (DEM) data were obtained from the Geospatial Data Cloud, which facilitated a deeper understanding of the interrelationships between topography and vegetation and provided crucial support for the analysis of structural equation modeling. Considering that the resolution of the radiation data in this study is 10 km, we set the spatial resolution at 1 km to ensure data consistency and avoid errors caused by

downscaling. All data were resampled to this uniform resolution, ensuring data uniformity for subsequent analyses.

2.3. Methods

The objective of this study is to elucidate the role of vegetation phenology in complex dryland ecosystems under the influence of climate change. The specific research focuses, and technical route are as follows: First, based on remote sensing and meteorological data, the Carnegie–Ames–Stanford Approach (CASA) model was constructed to estimate vegetation NPP at different time periods, revealing the evolution of vegetation productivity in the WSEFCA. NDVI was used to extract phenological information and analyze the characteristics of changes in the growing season of vegetation within the study area. Second, using Structural Equation Modeling (SEM), the contributions of climate and phenology to vegetation NPP changes were quantified, establishing a causal mechanism chain between climate, phenology and vegetation NPP. This clarified the pathways through which climate change impacts vegetation growth in arid regions and identified the dominant factors driving vegetation change. The technical route is shown in Figure 2.

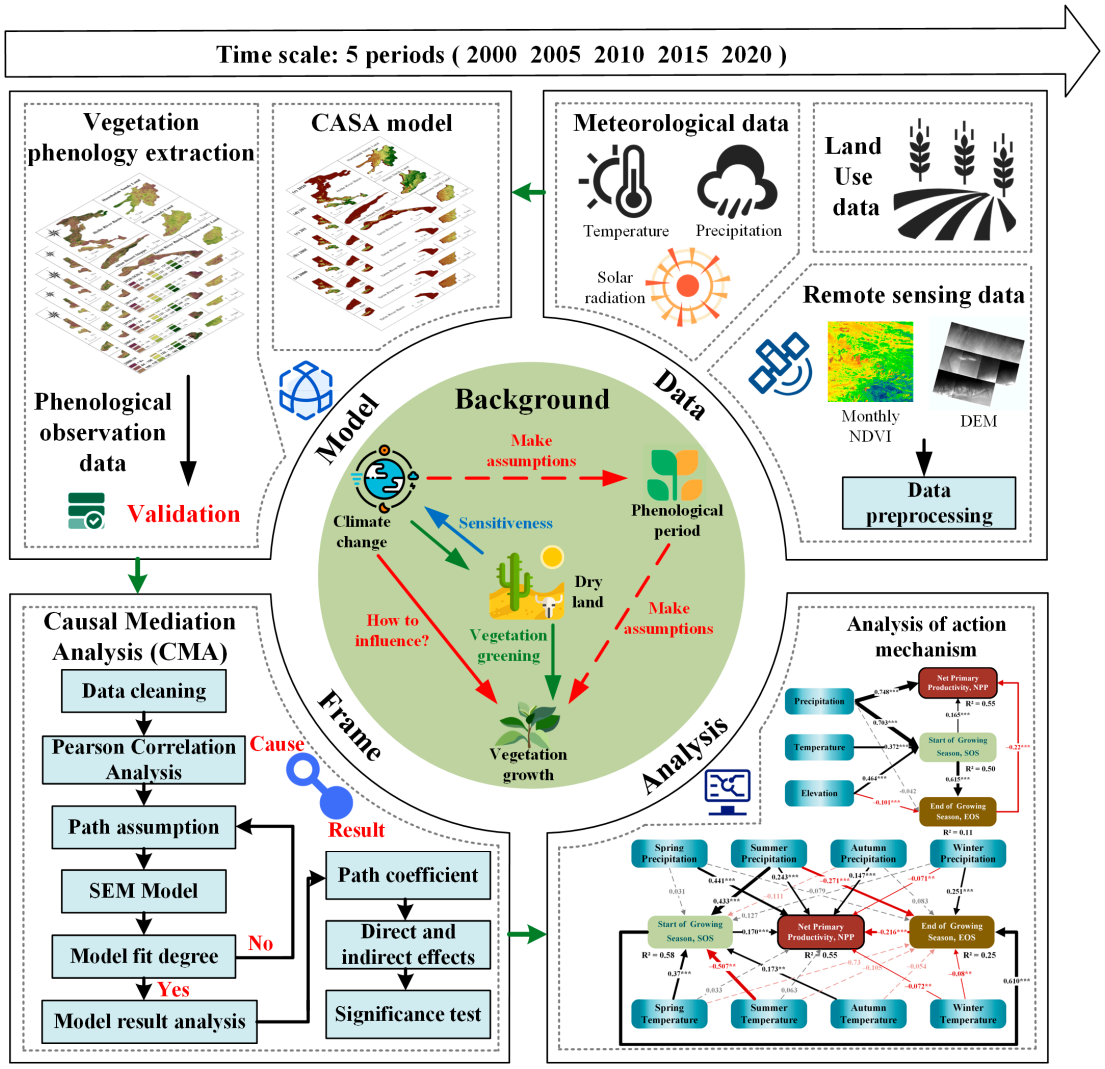

Figure 2. Technical route. (Analysis of action mechanism: The solid line indicates a significant relationship ($p < 0.05$), while the dashed line indicates a non-significant relationship. The black line indicates the positive paths, and the red line indicates the negative paths. The asterisks *** and ** indicate significance levels of 0.001 and 0.05).

2.3.1. Estimation of Vegetation NPP

In this study, we employed an improved light use efficiency model to estimate vegetation NPP, which is better suited to the conditions in China than the classical CASA model and has been extensively utilized in arid and semi-arid regions [32,33]. The NPP estimation model, based on remote sensing, was constructed based on the following variables: vegetation types, NDVI, temperature, precipitation and solar radiation data. The specific model construction process is as follows:

$$NPP(x,\ t) = APAR(x,\ t) \times \varepsilon(x,\ t) \quad (1)$$

In this equation, x represents the computational unit (pixel). t denotes the time scale (months). $APAR$ and ε are defined as photosynthetically active radiation absorbed by vegetation and the actual light use efficiency, respectively. The formulas for calculating $APAR$ (x, t) and ε (x, t) are as follows:

$$APAR(x,\ t) = SOL(x\ ,t) \times FPAR(x,\ t) \times 0.5 \quad (2)$$

$$\varepsilon(x,\ t) = T_{\varepsilon 1}(x,\ t) \times T_{\varepsilon 2}(x,\ t) \times \varepsilon_{max} \quad (3)$$

In this context, SOL and $FPAR$ represent the absorption rates of total solar radiation and incident photosynthetically active radiation by vegetation, respectively. $T_{\varepsilon 1}(x, t)$ and $T_{\varepsilon 2}(x, t)$ reflect the stress effects of low and high temperatures on light use efficiency. W_{ε} is the water stress coefficient, while ε_{max} denotes the maximum light energy utilization under ideal conditions, which varies in value depending on the vegetation type.

The global vegetation maximum light energy utilization [34] is not well-suited for the present study area. To ensure the accuracy of the model, we selected the simulated maximum light energy utilization data of Chinese vegetation types [35] for the calculation. In the subsequent study, the reliability of the model was further enhanced through the assurance that the number of rows and columns of the vegetation type data matched the meteorological raster data.

2.3.2. Information Extraction of Vegetation Phenology

In the process of extracting vegetation surface phenology, satellite remote sensing data were used as the primary source of information. However, as satellite data are affected by atmospheric conditions, cloud cover and other factors, they exhibit irregularities and abrupt changes, which present challenges to the accurate extraction of vegetation phenology [18]. The development of remote sensing technology has greatly improved the accuracy of vegetation phenology extraction [36,37]. To address these challenges, we employed the Savitzky–Golay (S–G) filtering method [38] to process the satellite remote sensing data into a smooth time series. The S-G filtering can retain both the position and peaks of the time series data while effectively eliminating noise in the data during the processing of the time series data [39]. The characteristics of this method render it optimal for processing satellite remote sensing data, thereby providing a more reliable and uniform foundation for subsequent vegetation phenology extraction.

$$Y_j = \frac{\sum_{i=-m}^{i=m} C_i Y_{j+1}}{N} \quad (4)$$

In this equation, Y_j represents the NDVI series data after smoothing, Y_{j+1} denotes the original NDVI time series data, C_i signifies the S-G filter coefficient and N represents the size of the sliding window.

The most utilized methodologies for the extraction of vegetation phenology data are primarily the threshold method and the maximum ratio method. In consideration of the operational feasibility and spatio-temporal applicability [40], the dynamic threshold method was employed for the extraction of climate parameters from the smoothed NDVI time series. Following the introduction of the dynamic thresholding method for climate

feature extraction, the recommendation of setting the threshold for SOS and EOS to 0.2 [41] was widely adopted by numerous climate researchers. However, the determination of thresholds is dependent on the specific plant species and geographical location in question, and therefore requires careful consideration during the selection process. Accordingly, a range of dynamic thresholds, spanning from 10% to 80%, were established in this study. The results were validated using ground monitoring data (Table 2), and the dynamic thresholds of 40% and 60% were ultimately selected for vegetation SOS and vegetation EOS, ensuring that the extracted climatic parameters were consistent with the actual ground conditions.

$$NDVI_{radio} = \frac{NDVI_t - NDVI_{min}}{NDVI_{max} - NDVI_{min}} \quad (5)$$

Table 2. Phenology (SOS and EOS) extracted from different thresholds (A1/A2) and ground-based monitoring data in 2015.

A1/A2	SOS	EOS
10%	87.71	321.95
20%	92.51	316.79
30%	105.85	306.74
40%	119.05	297.19
50%	129.54	287.73
60%	141.69	278.00
70%	154.55	267.48
80%	168.98	255.84
Ground monitoring data	122.81	278.14

In this equation, $NDVI_{radio}$ is the first year in which the threshold is exceeded, $NDVI_t$ is the NDVI value at a given time t, $NDVI_{max}$ and $NDVI_{min}$ are the maximum and minimum values in the annual cycle of the NDVI time series, respectively.

2.3.3. Analysis of Causal Mediation

SEM is a multivariate statistical technique used to analyze complex relationships between variables [42]. There are three key advantages of SEM over traditional regression analysis in mediation effects analysis. First, SEM permits the incorporation of measurement error into variables, thereby yielding more precise estimates than are possible with ordinary regression analysis. Second, SEM is capable of handling multiple dependent and multiple mediating variables simultaneously, facilitating the clear identification of the strength of each relationship. Finally, SEM quantitatively distinguishes between direct and indirect effects, thereby revealing the mediating mechanism. In recent years, SEM has been widely applied in ecological research [43]. Based on these advantages, we utilized SEM to quantify the mediating role of phenology between climate and vegetation NPP.

During the process of selecting model variables, we focused primarily on temperature and precipitation as the key climatic factors. This choice was not only supported by existing literature but also validated by the results of correlation analysis (Table 3). Although other climatic factors, such as wind speed, may also have some influence on vegetation growth, their relative impact was comparatively smaller and therefore not included in our model. This simplified design helps to concentrate on the main driving factors, thereby highlighting the direct regulatory effects of temperature and precipitation on NPP.

Table 3. Correlation analysis results (* significant at the 0.05 level, ** significant at the 0.01 level).

	Wind Speed	Temperature	SOS	Precipitation	NPP	EOS
Wind Speed	1.000	−0.108 *	0.061	−0.040	−0.013	−0.005
Temperature	−0.108 *	1.000	0.012	−0.291 **	−0.227 **	0.077
SOS	0.061	0.012	1.000	0.035	−0.084	0.639 **
Precipitation	−0.040	−0.291 **	0.035	1.000	0.613 **	0.045
NPP	−0.013	−0.277 **	−0.084	0.613 **	1.000	−0.056
EOS	−0.005	0.077	0.639 **	0.045	−0.056	1.000

If the model's fit was insufficient, the path assumptions were revised in accordance with the findings until the model achieved an acceptable level of fit. Once the SEM model was successfully developed, the total effects were decomposed into direct and indirect effects, and the significance of the indirect effects was tested using the Bootstrap method [44]. This allowed us to uncover both the causal relationships and the mediating mechanisms. Figure 3 illustrates the workflow for developing the vegetation NPP change mechanism.

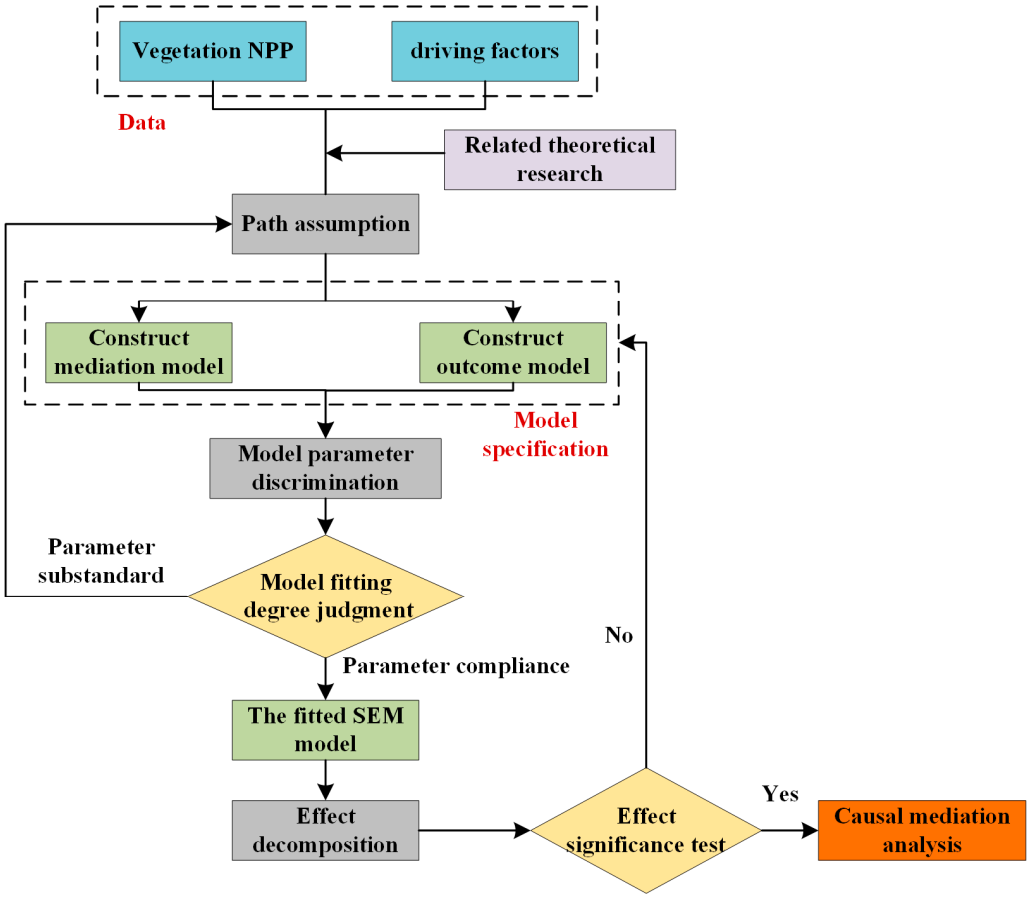

Figure 3. Model diagram of the driving mechanism of vegetation NPP change in the WSEFCA.

2.3.4. Data Statistics and Analysis

In this study, we conducted a statistical analysis of variables such as temperature, precipitation and NDVI to provide climate context and data support. According to Table 4, the annual average precipitation is 16.37 mm, with a standard deviation of 13.224, indicating significant temporal and spatial variability in precipitation. The maximum precipitation recorded was 53.54 mm in 2010, while the minimum was 0.61 mm in 2020. The annual average temperature is 6.616 °C, with a standard deviation of 3.828, showing relatively stable fluctuations over time. The lowest temperature recorded was −5.424 °C in 2000,

and the highest was 13.45 °C in 2020. The annual average NDVI is 0.1092, with a standard deviation of 0.1676; the maximum value is 0.6218 and the minimum is −0.1956, indicating relatively stable changes in vegetation cover in the region. Additionally, the average DEM of the study area is 1574.127 m, with a standard deviation of 1176.76 m, reflecting significant topographic variability in the region.

Table 4. Statistical results of selected raw data.

	Year	Maximum	Minimum	Mean	Standard Deviation
Precipitation (mm)	2000	1.34	47.57	15.011	11.021
	2005	2.073	49.575	15.293	11.952
	2010	1.104	53.538	17.402	13.942
	2015	1.518	40.80	16.515	12.976
	2020	0.61	48.461	17.624	16.23
annual average		1.329	47.9888	16.369	13.2242
Temperature (degree centigrade)	2000	−5.424	13.26	6.42	3.88
	2005	−5.41	13.61	6.77	3.79
	2010	−5.4	13.2	6.28	3.74
	2015	−5.4	13.72	6.69	3.89
	2020	−5.17	13.45	6.92	3.84
annual average		−5.3608	13.448	6.616	3.828
NDVI	2000	−0.196	0.53	0.1	0.06
	2005	−0.196	0.6	0.11	0.06
	2010	−0.194	0.646	0.106	0.057
	2015	−0.2	0.658	0.11	0.595
	2020	−0.192	0.675	0.12	0.066
annual average		−0.1956	0.6218	0.1092	0.1676
DEM (m)		66	6063	1574.127	1176.76

These statistical analyses provide essential data support for subsequent in-depth studies on the impacts of climate change, vegetation NPP and phenological changes.

3. Results

3.1. Characteristics of Spatial and Temporal Changes of NPP in Typical Ecological Function Reserve Areas

The NPP of WSEFCA showed a significant upward trend over the past two decades, with the average value rising from 55.55 gC/(m^2·a) in 2000 to 75.01 gC/(m^2·a) in 2020 (Figure 4). The long-term pattern of vegetation NPP indicates a gradual improvement in the ecological condition in the WSEFCA, particularly in the Hunsandak and Horqin.

As the ecological restoration efforts progressed, a noticeable diversification in the spatial distribution of NPP became evident (Figure 4A). However, the NPP levels in the Altun, the Tarim and the northern part of the Heihe remain relatively low, with values ranging between 0 and 90 gC/(m^2·a). However, an increase in NPP was observed in some regions in 2010 and 2015. For instance, at the southeastern border of the Hunsandak and Maowusu, the vegetation NPP gradually shifted from low to medium-high levels, exceeding 200 gC/(m^2·a) in most areas. Meanwhile, the Horqin demonstrated a sustained high level of vegetation NPP.

With regard to seasonal fluctuations, the annual mean NPP in each region exhibited a discernible upward trajectory from 2000 to 2020. This trend was particularly pronounced during the summer months, when the mean vegetation NPP reached its highest point and demonstrated a consistent annual increase, consistently remaining above 10 gC/(m^2·a). By 2020, the mean summer vegetation NPP had reached 15.11 gC/(m^2·a) (Figure 4B). This highlights the significant influence of seasonal variations on vegetation growth. However, the changes in vegetation NPP among different regions showed significant variation (Figure 4C).

The highest annual mean vegetation NPP was recorded in the Horqin, followed by the Hunsandak and the Maowusu, which demonstrated a substantial enhancement of NPP across all three regions. In comparison, the vegetation NPP in the Tarim, Altun and Heihe exhibited minimal alteration and lower mean values, suggesting that the ecological environment of these regions situated in northwestern China still requires further enhancement.

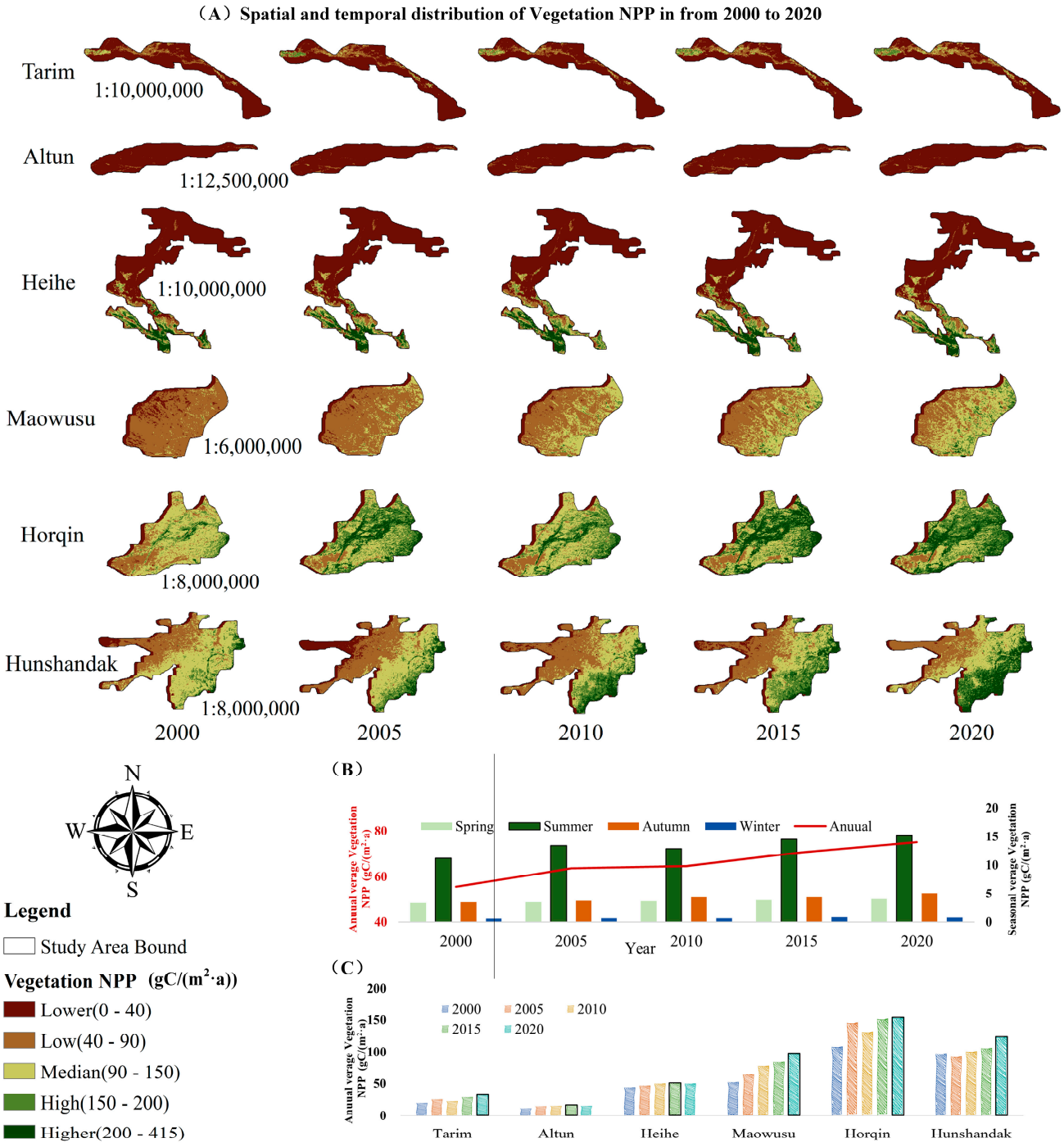

Figure 4. Spatial and temporal evolution of vegetation NPP ((**A**) spatial pattern of vegetation NPP in the study area in 2000, 2005, 2010, 2015 and 2020; (**B**) changes in vegetation NPP in different years and seasons; and (**C**) changes in vegetation NPP in different regions (black lines indicate the years with the highest values).

3.2. Spatial and Temporal Characteristics of Vegetation Climatic Changes

From 2000 to 2020, the vegetation SOS in the WSEFCA exhibited a spatial pattern of gradual delay from east to west (Figure 5A). Significant differences in SOS were observed among regions. The Tarim and the Altun showed an overall trend of advancement, while the Horqin and the Maowusu exhibited the opposite pattern, with SOS gradually advancing as longitude increases. In contrast, the SOS in the Hunshandake and the northern part of the Heihe has shown a delaying trend, reflecting the different climate responses in these regions.

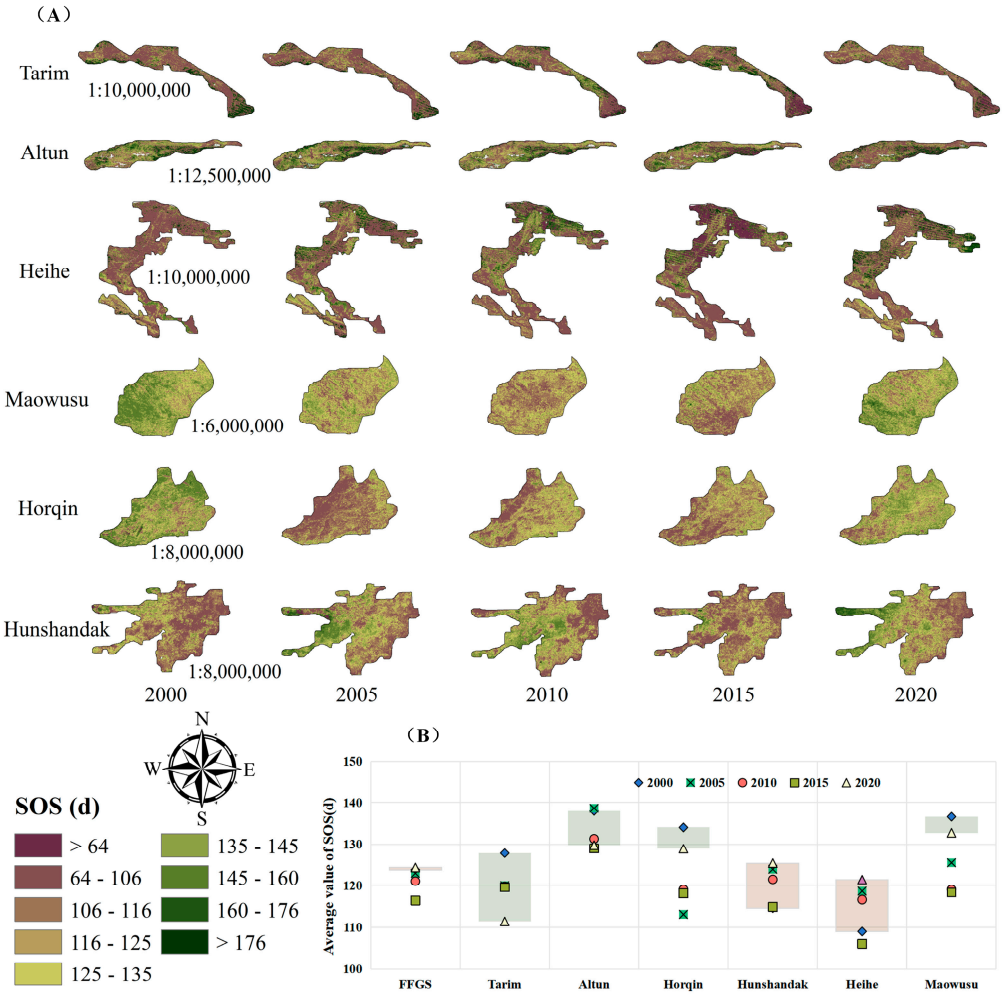

Figure 5. Spatial and temporal evolution of SOS. (**A**) Spatial patterns of vegetation SOS in the study area for the years 2000, 2005, 2010, 2015 and 2020. (**B**) Changes in vegetation SOS in different regions (green boxes represent advancing times, orange represents delaying times).

The spatial pattern of EOS showed similarities to that of SOS, yet also demonstrated regional specificity (Figure 6A). In the Tarim, the advancement of EOS is particularly pronounced, especially in the northwestern and southeastern regions. Meanwhile, the overall change in the Hunshandake is relatively stable; however, a significant delay in EOS was observed in the northeastern part in 2015. By comparison, the changes in EOS in the Horqin and the Maowusu are relatively minor. These discrepancies illustrate the varying effects of climate change on vegetation phenology across diverse topographic regions.

The interannual variation of SOS and EOS exhibits complexity within the subregions (Figures 5B and 6B). In the Tarim and Altun, both SOS and EOS demonstrated notable advancement, with SOS advancing by approximately 2 to 3 days and EOS advancing by 10 to 15 days per decade on average. The trend of SOS and EOS in the Horqin and Mauwusu

was consistent, with advancement followed by postponement. In contrast, the mean values of SOS in the Heihe and the Hunsandak exhibited a relatively stable 10-day difference over the 20-year period.

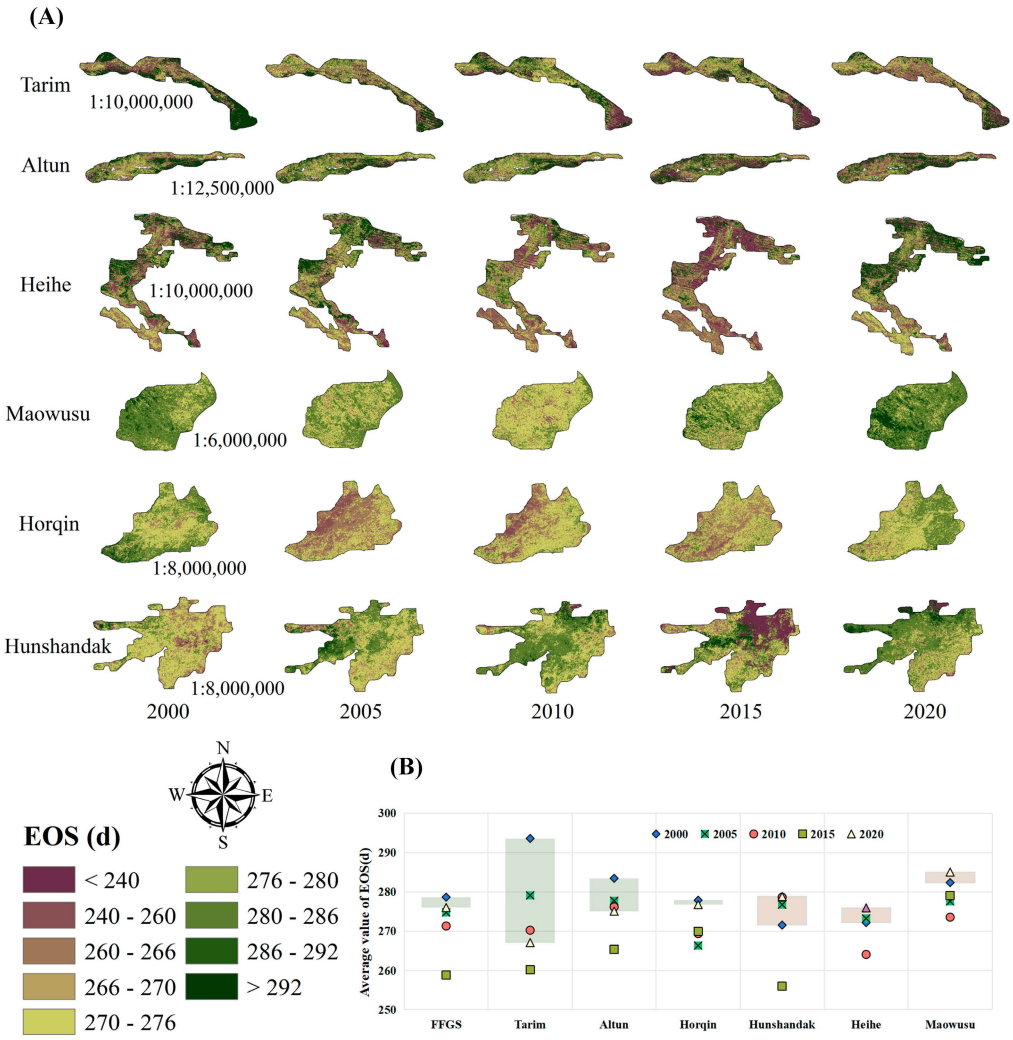

Figure 6. Spatial and temporal evolution of EOS. (**A**) Spatial patterns of vegetation EOS in the study area for the years 2000, 2005, 2010, 2015 and 2020. (**B**) Changes in vegetation EOS in different regions (green boxes represent advancing times, orange represents delaying times).

3.3. Influence Pathways of Climate and Phenology Changes on Vegetation NPP Changes

The final model fitted by SEM is shown in Figure 7. This model provides effectively captures the interactions among the variables and reveals the pathways through which climatic factors influence vegetation NPP across multiple temporal scales (annual and seasonal). The model showed strong goodness of fit at both the annual and seasonal scales (Table 5), indicating robust explanatory power.

Table 5. Fitting of the model.

	CHISQ	GFI	CFI	RMR	SRMR	RMSEA
Annual scale	0.036	0.998	0.999	0.014	0.007	0.034
Seasonal scale	0.103	0.997	0.998	0.019	0.01	0.021

First, the pathways of climate change effects on vegetation NPP exhibited a significant relationship from an annual scale perspective (Appendix A, Figure A1). The mean annual

precipitation had a strongly significant effect on SOS and NPP ($p < 0.001$), but not on EOS ($p > 0.05$). Furthermore, precipitation indirectly increased NPP via its influence (with an indirect effect of 0.116 and a total effect amounting to 0.819). Although the direct effect of precipitation on EOS was not significant, the total effect of precipitation on EOS was 0.432, as indicated by the indirect effect of SOS on EOS (Appendix A, Table A1). Meanwhile, EOS exhibited a significant negative direct effect on NPP (with an impact coefficient of −0.220). Although DEM lacked a direct effect on NPP alterations, it exerted a modest total effect on NPP via the indirect influences of SOS and EOS (with indirect effects of 0.077 and 0.022, respectively).

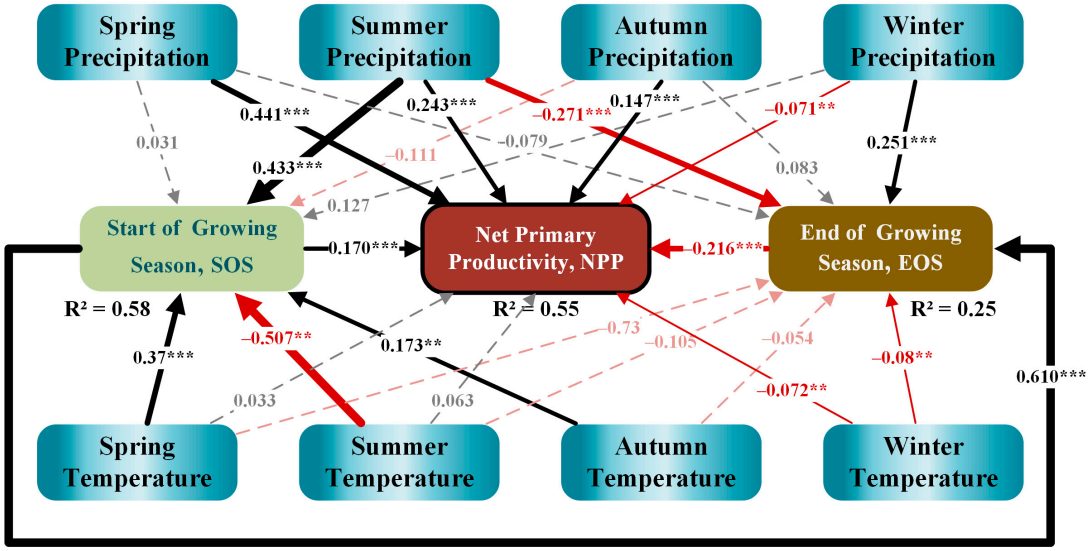

Figure 7. The relationships between climatic factors and NPP, SOS and EOS on seasonal scales. The values on the lines represent standardized throughput coefficients, and the thickness of the arrows indicates the magnitude of the standardized coefficients. A solid line indicates a significant relationship ($p < 0.05$), while a dashed line indicates a non-significant relationship. Black lines indicate positive paths, and red lines indicate negative paths. The asterisks *** and ** indicate significance levels of 0.001 and 0.05, respectively. R^2 denotes the degree of coexplanation of the variable in question.

The patterns observed at the annual scale demonstrated a greater complexity of influence at the seasonal scale (Figure 7). Spring precipitation exerts a considerable direct influence on NPP, with an effect coefficient of 0.441. This represents one of the most pronounced direct effects of seasonal precipitation on NPP variability. This indicates that spring precipitation plays a crucial role in regulating NPP. The impact of summer precipitation on NPP was more intricate. It exerted a direct effect of 0.243 and also exerted an indirect influence on NPP alterations through a substantial positive effect on SOS (with an impact coefficient of 0.433) and a negative effect on EOS (with an impact coefficient of −0.271). This indirect effect was 0.133, indicating that the contribution of summer precipitation is influenced by the combined effects of multiple pathways, exhibiting a complex pattern of indirect effects. The direct effect of fall and winter precipitation on NPP was smaller, with values of 0.147 and −0.071, respectively. Additionally, the indirect effect of winter precipitation on NPP through the EOS was −0.054, resulting in a total effect of −0.125 (Table 6). This further demonstrates that the negative impact of winter precipitation on NPP is indirectly mediated through the EOS pathway.

Another crucial climatic factor, temperature, also exerted diverse influences on NPP at varying temporal scales. The mean annual air temperature exhibited a highly significant direct effect on SOS ($p < 0.001$, with an effect coefficient of 0.372), whereas seasonal air temperature effects demonstrated more nuanced differences. For example, summer

temperatures had a significant negative effect on SOS ($p < 0.05$, with an impact coefficient of −0.507). In contrast, the positive effects of spring and fall temperatures on SOS indirectly supported NPP growth, reflecting that temperature changes in different seasons have varying regulatory effects on vegetation growth.

Table 6. Results of direct, indirect and total effects of seasonal changes in temperature, precipitation, SOS, EOS and NPP (slash indicates no indirect effect, NS indicates that the pathway is not significant, spring precipitation (PRE-Spring), spring temperatures (TEMP-Spring)).

Paths	Direct Effects	Paths	Indirect Effects	Paths	Total Effects
PRE-Spring → NPP	0.441	/	/	PRE-Spring → NPP	0.441
PRE-Summer → SOS	0.433	PRE-Summer → SOS → NPP	0.074	PRE-Summer → SOS	0.433
PRE-Summer → EOS	−0.271	PRE-Summer → EOS → NPP	0.059	PRE-Summer → EOS	−0.007
PRE-Summer → NPP	0.243	PRE-Summer → SOS → EOS	0.264	PRE-Summer → NPP	0.376
PRE-Autumn → NPP	0.147	/	/	PRE-Autumn → NPP	0.147
PRE-Winter → EOS	0.251	PRE-Winter → EOS → NPP	−0.054	PRE-Winter → EOS	0.251
PRE-Winter → NPP	−0.071			PRE-Winter → NPP	−0.125
TEMP-Spring → SOS	0.37	TEMP-Spring → SOS → NPP	0.063	TEMP-Spring → SOS	0.37
TEMP-Spring → NPP	NS			TEMP-Spring → NPP	0.063
TEMP-Summer → SOS	−0.507	TEMP-Summer → SOS → NPP	−0.086	TEMP-Summer → SOS	0.37
TEMP-Summer → NPP	NS			TEMP-Summer → NPP	−0.086
TEMP-Autumn → SOS	0.173	TEMP-Autumn → SOS → NPP	0.029	TEMP-Autumn → SOS	0.173
TEMP-Autumn → NPP	NS			TEMP-Autumn → NPP	0.029
TEMP-Winter → EOS	−0.08	TEMP-Winter → EOS → NPP	0.016	TEMP-Winter → EOS	−0.072
TEMP-Winter → NPP	−0.072			TEMP-Winter → NPP	−0.064
SOS → EOS	0.610	SOS → EOS → NPP	−0.132	SOS → EOS	0.610
SOS → NPP	0.170	/	/	SOS → NPP	0.038
EOS → NPP	−0.216	/	/	EOS → NPP	−0.216

4. Discussion

This study reveals the spatial and temporal characteristics of the NPP of vegetation in the WSEFCA over the past two decades. Overall, vegetation NPP has exhibited a significant upward trend, which was closely related to changes in climatic conditions within the region. In particular, the increase in vegetation NPP was especially in years when precipitation increased precipitation, indicating that precipitation is the primary driving factor influencing vegetation productivity [28]. However, when both precipitation and temperature are considered together, the increase in NPP is not uniform. In fact, significant differences are observed between seasons and regions. For example, the NPP elevation in the Hunsandak, Maowusu and Horqin was particularly significant in years of relatively abundant precipitation. The climate conditions in these regions are relatively mild, with abundant rainfall, reaching over 300 mm annually. As a result, the vegetation in these areas is highly responsive to water availability, which promotes vegetation recovery [45–47]. In contrast, in regions with high temperatures and low precipitation, such as the Tarim River Basin and the Arjin Desert Steppe, the increase in NPP was relatively modest, and the overall level remained low. The ecosystem recovery in these regions is relatively delayed, with extreme high temperatures and high evaporation rates severely limiting plant growth. In the Tarim River Basin, summer temperatures often exceed 40 °C, while annual rainfall is less than 50 mm. These extreme climatic conditions directly contribute to the low level of vegetation productivity in the area [48,49]. Similarly, the Heihe River Basin exhibited comparable outcomes, further indicating that in the arid regions of northwestern China, NPP levels are typically low and highly susceptible to precipitation fluctuations due to a significant scarcity of water resources [50]. Recent studies have also shown that vegetation growth in these arid regions is more severely affected by climate change, with extreme precipitation events posing additional challenges to ecosystem recovery [51,52].

Further exploring the impact of climate change and phenological changes on NPP, this study reinforces the necessity of comprehending the interdependent relationships between climate, phenology and vegetation. It has been demonstrated that there are notable differences in the impact of climatic variables on vegetation phenology across different seasons. To illustrate,

spring temperature has been demonstrated to exert a pronounced influence on SOS, whereas fall precipitation has been shown to exert a significant impact on EOS [7,8]. This seasonal difference has been validated to varying degrees in arid and semi-arid regions around the world, thereby confirming the critical role of climatic factors on vegetation growth [5,53]. The results demonstrated that the impact of climatic factors on SOS is generally more pronounced than that on EOS. The positive effect of warmer spring temperatures on SOS is observed to be driven by the promotion of early vegetation emergence and growth, which in turn led to an increase in NPP. However, the rise in summer temperatures has a significant negative effect on SOS. It is found that higher temperatures potentially led to an earlier growing season, which in turn inhibited NPP accumulation by shortening the growing season. While warmer temperatures often facilitate early growth, in extreme climatic conditions, this advancement may negatively impact NPP on an annual basis [9]. Recent literature also supports this view, suggesting that extreme climate events may have a significant impact on vegetation phenology and weaken the potential for NPP growth [54]. Additionally, the rise in precipitation has a considerable positive impact on SOS, yet a detrimental effect on EOS. This suggests that, while increased precipitation typically fosters vegetation growth, excessive precipitation may alternatively precipitate water stress in arid ecosystems, thereby constraining vegetation expansion [55,56]. This underscores that the impact of phenological shifts on NPP is not solely contingent on the overall precipitation levels but is also profoundly shaped by the cumulative effect of local precipitation patterns and climate variability.

Furthermore, the prolongation of vegetation phenology resulting from climate change may augment NPP in the immediate term. However, in the long term, recurrent extreme climatic occurrences may offset this impact, particularly in regions characterised by elevated climate variability [57]. This intricate dynamic indicates that future research must prioritize investigating the direct and indirect impacts of climate change on phenological events. A multi-scale and multi-factor analysis approach will facilitate a more comprehensive understanding of the mechanisms through which climate change affects NPP, thereby providing a scientific foundation for the management and restoration of ecosystems.

The results demonstrated that the duration of the vegetation growing season was progressively extended with the intensification of seasonal precipitation and temperature fluctuations, which led to an increase in vegetation NPP. However, ecosystems may experience heightened levels of water stress and heat stress as summer temperatures continue to rise and precipitation patterns become increasingly erratic [58,59]. In dryland ecosystems, there is considerable spatial heterogeneity in temperature and precipitation, with a high degree of uncertainty [22]. It is therefore imperative that future ecological restoration strategies give special consideration to the potential challenges posed by water carrying capacity and seasonal climate change in these regions. The spatial distribution of water and heat is significantly influenced by local topography and soil conditions, thereby increasing the complexity of ecological restoration. In order to effectively address the uncertainties posed by future climate change, ecological restoration strategies must prioritize nature-based solutions and incorporate a comprehensive assessment of the dual impacts of local climate variability on vegetation growth. In particular, when considering the restoration of windbreaks in future climate scenarios, it is essential to address both the enhancement of plant water use efficiency and the sustainable management of soil moisture. It is imperative to increase ground cover in order to enhance soil moisture retention and to adapt to climate change by optimizing vegetation structure. Furthermore, in regions experiencing prolonged periods of drought, it is essential to implement more adaptive vegetation-restoration strategies that prioritize the introduction of drought-tolerant species and the effective management of water resources. This approach is crucial to ensure the long-term resilience and stability of the ecosystem. Furthermore, future restoration strategies should prioritize the monitoring of vegetation phenology dynamics under climate change scenarios, with a particular emphasis on the study of response mechanisms to seasonal climate change.

Although this study focuses on the effects of climatic and phenological changes on vegetation growth, while the effects of human activities are relatively less addressed. Anthropogenic activities exert a more pronounced influence on vegetation cover (e.g., ecological restoration projects) within the study area. However, a more comprehensive investigation is required to elucidate the precise nature of these impacts. Subsequent studies will investigate the role of human activities in ecological restoration in greater detail, particularly in the context of interactions with climate change. This will provide a crucial foundation for the development of more precise and sustainable restoration strategies.

5. Conclusions

This study focuses on WSEFCA, utilizing an SEM model to construct a relational network that quantitatively evaluates the impact of climatic factors and phenological events on vegetation NPP. It reveals the crucial role phenology plays in climate-driven NPP changes under arid and semi-arid conditions. The results indicate that while the overall ecological environment of these conservation areas has improved, significant regional disparities persist, particularly in northwestern China, where further ecological improvements are needed. In the arid and semi-arid regions, summer precipitation notably advances spring SOS and delays autumn EOS, thereby indirectly enhancing the growth potential of vegetation NPP. The study further demonstrates that climate change indirectly influences vegetation growth cycles and productivity by regulating phenological events.

This research provides a basis for formulating more precise strategies for ecological protection and restoration. In other similar arid regions, ecological restoration efforts should also focus on the relationship between regional climate and phenological changes, in order to develop location-specific strategies to address the impact of climate change on vegetation productivity. Future ecological management strategies should fully consider the regulatory effects of climate change on phenology and NPP to effectively address the challenges of ecological restoration in global arid zones.

Author Contributions: X.L.: Data curation, Formal analysis, Methodology, Software, Writing—original draft. H.L.: Conceptualization, Funding acquisition, Methodology, Resources, Writing—review and editing. Y.Z.: Conceptualization, Project administration, Validation, Writing—review and editing. Y.Y.: Data curation, Formal analysis, Software. X.W.: Investigation, Project administration, Supervision. All authors have read and agreed to the published version of the manuscript.

Funding: This research was funded by The Key Projects of Jiangxi Natural Science Foundation, grant number 20232ACB203025, and the Science and Technology Project of the Jiangxi Provincial Department of Natural Resources, grant number ZRKJ20232523.

Institutional Review Board Statement: Not applicable.

Informed Consent Statement: Not applicable.

Data Availability Statement: Data derived from public domain resources.

Conflicts of Interest: The authors declare no conflicts of interest.

Appendix A

Table A1. Results of direct, indirect, and total effects of annual changes in temperature, precipitation, SOS, EOS, and NPP (slashes indicate no indirect effects, NS indicates the path is not significant).

Paths	Direct Effects	Paths	Indirect Effects	Paths	Total Effects
PRE → SOS	0.703	PRE → SOS → NPP	0.116	PRE → SOS	0.703
PRE → EOS	NS	PRE → EOS → NPP	NS	PRE → EOS	0.432
PRE → NPP	0.748	PRE → SOS → EOS	0.432	PRE → NPP	0.819
TEMP → SOS	0.372	TEMP → SOS → NPP	0.061	TEMP → SOS	0.372
		TEMP → SOS → EOS	0.229	TEMP → EOS	0.229
				TEMP → SOS	0.061

Table A1. *Cont.*

Paths	Direct Effects	Paths	Indirect Effects	Paths	Total Effects
DEM → SOS	0.464	DEM → SOS → EOS	0.285	DEM → SOS	0.464
DEM → EOS	−0.101	DEM → SOS → NPP	0.077	DEM → EOS	0.149
		DEM → EOS → NPP	0.022	DEM → NPP	0.099
SOS → EOS	0.615	SOS → EOS → NPP	−0.135	SOS → EOS	0.615
SOS → NPP	0.165			SOS → NPP	0.030
EOS → NPP	−0.220	/		EOS → NPP	−0.220

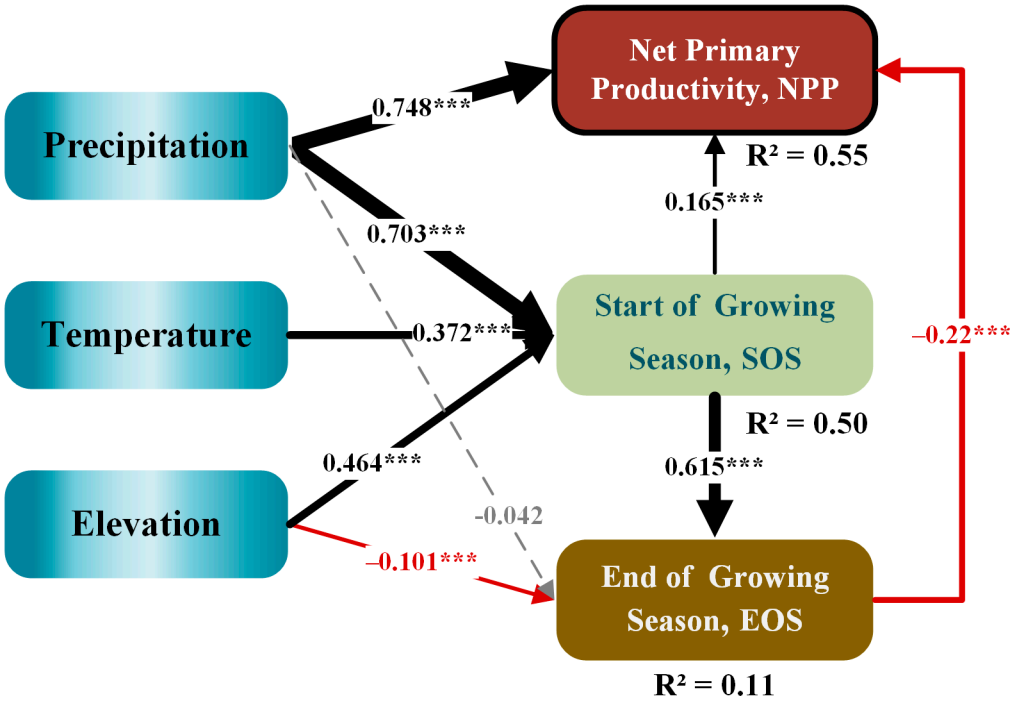

Figure A1. The relationships between climatic factors and NPP, SOS, and EOS on annual scales. The values on the lines represent standardized throughput coefficients, and the thickness of the arrows indicates the magnitude of the standardized coefficients. A solid line indicates a significant relationship ($p < 0.05$), while a dashed line indicates a non-significant relationship. Black lines indicate positive paths, and red lines indicate negative paths. The asterisks *** indicate a significance level of 0.001. R^2 denotes the degree of coexplanation of the variable in question.

References

1. Field, C.B.; Behrenfeld, M.J.; Randerson, J.T.; Falkowski, P. Primary production of the biosphere: Integrating terrestrial and oceanic components. *Science* **1998**, *281*, 237–240. [CrossRef] [PubMed]
2. Li, H.; Wu, Y.; Liu, S.; Xiao, J. Regional contributions to interannual variability of net primary production and climatic attributions. *Agric. For. Meteorol.* **2021**, *303*, 108384. [CrossRef]
3. Poulter, B.; Frank, D.; Ciais, P.; Myneni, R.B.; Andela, N.; Bi, J.; Broquet, G.; Canadell, J.G.; Chevallier, F.; Liu, Y.Y.; et al. Contribution of semi-arid ecosystems to interannual variability of the global carbon cycle. *Nature* **2014**, *509*, 600–603. [CrossRef] [PubMed]
4. Wang, S.; Fu, B.; Wei, F.; Piao, S.; Maestre, F.T.; Wang, L.; Jiao, W.; Liu, Y.; Li, Y.; Li, C.; et al. Drylands contribute disproportionately to observed global productivity increases. *Sci. Bull.* **2023**, *68*, 224–232. [CrossRef] [PubMed]
5. Li, J.; Liu, L.; Zheng, J.; Yu, X.; Tian, R.; Han, W.; Guan, J. Increasing influence of minimum temperature on grassland spring phenology in arid Central Asia. *Agric. For. Meteorol.* **2024**, *355*, 110122. [CrossRef]
6. Lyu, J.; Fu, X.; Lu, C.; Zhang, Y.; Luo, P.; Guo, P.; Huo, A.; Zhou, M. Quantitative assessment of spatiotemporal dynamics in vegetation NPP, NEP and carbon sink capacity in the Weihe River Basin from 2001 to 2020. *J. Clean. Prod.* **2023**, *428*, 139384. [CrossRef]
7. Li, C.; Wang, R.; Cui, X.; Wu, F.; Yan, Y.; Peng, Q.; Qian, Z.; Xu, Y. Responses of vegetation spring phenology to climatic factors in Xinjiang, China. *Ecol. Indic.* **2021**, *124*, 107286. [CrossRef]

8. Jiang, Q.; Yuan, Z.; Yin, J.; Yao, M.; Qin, T.; Lü, X.; Wu, G. Response of vegetation phenology to climate factors in the source region of the Yangtze and Yellow Rivers. *J. Plant Ecol.* **2024**, *17*, rtae046. [CrossRef]
9. Ji, Z.; Wang, L. Differential responses of vegetation phenology to climatic elements during extreme events on the Chinese loess plateau. *Sci. Total Environ.* **2024**, *933*, 173146. [CrossRef]
10. Mou, C.; Sun, G.; Luo, P.; Wang, Z.; Luo, G. 4Flowering Responses of Alpine Meadow Plant in the Qinghai-Tibetan Plateau to Extreme Drought Imposed in Different Periods. *Chin. J. Appl. Environ. Biol.* **2013**, *19*, 272–279. [CrossRef]
11. Chen, L.; Hänninen, H.; Rossi, S.; Smith, N.G.; Pau, S.; Liu, Z.; Feng, G.; Gao, J.; Liu, J. Leaf senescence exhibits stronger climatic responses during warm than during cold autumns. *Nat. Clim. Change* **2020**, *10*, 777–780. [CrossRef]
12. Kang, X.; Hao, Y.; Cui, X.; Chen, H.; Huang, S.; Du, Y.; Li, W.; Kardol, P.; Xiao, X.; Cui, L. Variability and changes in climate, phenology, and gross primary production of an alpine Wetland ecosystem. *Remote Sens.* **2016**, *8*, 391. [CrossRef]
13. Richardson, A.D.; Black, T.A.; Ciais, P.; Delbart, N.; Friedl, M.A.; Gobron, N.; Hollinger, D.Y.; Kutsch, W.L.; Longdoz, B.; Luyssaert, S.; et al. Influence of spring and autumn phenological transitions on forest ecosystem productivity. *Philos. Trans. R. Soc. B Biol. Sci.* **2010**, *365*, 3227–3246. [CrossRef] [PubMed]
14. Chen, C.; Park, T.; Wang, X.; Piao, S.; Xu, B.; Chaturvedi, R.K.; Fuchs, R.; Brovkin, V.; Ciais, P.; Fensholt, R.; et al. China and India lead in greening of the world through land-use management. *Nat. Sustain.* **2019**, *2*, 122–129. [CrossRef]
15. Xu, L.; Gao, G.; Wang, X.; Fu, B. Distinguishing the effects of climate change and vegetation greening on soil moisture variability along aridity gradient in the drylands of northern China. *Agric. For. Meteorol.* **2023**, *343*, 109786. [CrossRef]
16. Jie, X.; Yu, X.; Gaodi, X.; Yangyang, W.; Yuan, J.; Wenhui, C. Assessment of wind erosion prevention service and its beneficiary areas identification of national key ecological function zone of windbreak and sand fixation type in China. *Acta Ecol. Sin.* **2019**, *39*, 5857–5873. [CrossRef]
17. Li, H.; Feng, J.; Bai, L.; Zhang, J. Populus euphratica Phenology and Its Response to Climate Change in the Upper Tarim River Basin, NW China. *Forests* **2021**, *12*, 1315. [CrossRef]
18. Han, H.; Bai, J.; Ma, G.; Yan, J.; Wang, X.; Ta, Z.; Wang, P. Seasonal responses of net primary productivity of vegetation to phenological dynamics in the Loess Plateau, China. *Chin. Geogr. Sci.* **2022**, *32*, 340–357. [CrossRef]
19. Kang, W.; Wang, T.; Liu, S. The response of vegetation phenology and productivity to drought in Semi-Arid regions of northern China. *Remote Sens.* **2018**, *10*, 727. [CrossRef]
20. Liu, Z.; Liu, Y.; Li, Y. Extended warm temperate zone and opportunities for cropping system change in the Loess Plateau of China. *Int. J. Climatol.* **2018**, *39*, 658–669. [CrossRef]
21. Wu, L.; Ma, X.; Dou, X.; Zhu, J.; Zhao, C. Impacts of climate change on vegetation phenology and net primary productivity in arid Central Asia. *Sci. Total Environ.* **2021**, *796*, 149055. [CrossRef] [PubMed]
22. Smith, W.K.; Dannenberg, M.P.; Yan, D.; Herrmann, S.; Barnes, M.L.; Barron-Gafford, G.A.; Biederman, J.A.; Ferrenberg, S.; Fox, A.M.; Hudson, A.; et al. Remote sensing of dryland ecosystem structure and function: Progress, challenges, and opportunities. *Remote Sens. Environ.* **2019**, *233*, 111401. [CrossRef]
23. Hayes, A.F.; Montoya, A.K.; Rockwood, N.J. The Analysis of Mechanisms and Their Contingencies: PROCESS versus Structural Equation Modeling. *Australas. Mark. J.* **2017**, *25*, 76–81. [CrossRef]
24. Schweiger, E.W.; Grace, J.B.; Cooper, D.; Bobowski, B.; Britten, M. Using structural equation modeling to link human activities to wetland ecological integrity. *Ecosphere* **2016**, *7*, e01548. [CrossRef]
25. Ren, L.; Li, J.; Li, C.; Dang, P. Can ecotourism contribute to ecosystem? Evidence from local residents' ecological behaviors. *Sci. Total Environ.* **2021**, *757*, 143814. [CrossRef] [PubMed]
26. Chen, M.; Xue, Y.; Xue, Y.; Peng, J.; Guo, J.; Liang, H. Assessing the effects of climate and human activity on vegetation change in Northern China. *Environ. Res.* **2024**, *247*, 118233. [CrossRef] [PubMed]
27. Liu, B.; Tang, Q.; Zhou, Y.; Zeng, T.; Zhou, T. The Sensitivity of Vegetation Dynamics to Climate Change across the Tibetan Plateau. *Atmosphere* **2022**, *13*, 1112. [CrossRef]
28. Ling, H. Spatio-temporal dynamics of vegetation in key ecological function zone of wind-break and sand-fixation over the last 20 years. *Acta Ecol. Sin.* **2021**, *41*, 8341–8351. [CrossRef]
29. Harris, I.; Osborn, T.J.; Jones, P.; Lister, D. Version 4 of the CRU TS monthly high-resolution gridded multivariate climate dataset. *Sci. Data* **2020**, *7*, 109. [CrossRef]
30. Xue, C.; Wu, H.; Jiang, X. Temporal and Spatial Change Monitoring of Drought Grade Based on ERA5 Analysis Data and BFAST Method in the Belt and Road Area during 1989–2017. *Adv. Meteorol.* **2019**, *2019*, 4053718. [CrossRef]
31. Zhou, Y.; Liu, J. A MODIS EVI based dataset of vegetation phenology for the key ecological observation stations in China (2001–2016) [Dataset]. *Sci. Data Bank* **2017**. [CrossRef]
32. Yin, C.; Luo, M.; Meng, F.; Sa, C.; Yuan, Z.; Bao, Y. Contributions of climatic and anthropogenic drivers to net primary productivity of vegetation in the Mongolian Plateau. *Remote Sens.* **2022**, *14*, 3383. [CrossRef]
33. He, T.; Dai, X.; Li, W.; Zhou, J.; Zhang, J.; Li, C.; Dai, T.; Li, W.; Lu, H.; Ye, Y.; et al. Response of net primary productivity of vegetation to drought: A case study of Qinba Mountainous area, China (2001–2018). *Ecol. Indic.* **2023**, *149*, 110148. [CrossRef]
34. Potter, C.S.; Randerson, J.T.; Field, C.B.; Matson, P.A.; Vitousek, P.M.; Mooney, H.A.; Klooster, S.A. Terrestrial ecosystem production: A process model based on global satellite and surface data. *Glob. Biogeochem. Cycles* **1993**, *7*, 811–841. [CrossRef]
35. Zhu, W.; Pan, Y.; He, H.; Yu, D.; Hu, H. Simulation of maximum light use efficiency for some typical vegetation types in China. *Chin. Sci. Bull.* **2006**, *51*, 457–463. [CrossRef]

36. Kong, D.; McVicar, T.R.; Xiao, M.; Zhang, Y.; Peña-Arancibia, J.L.; Filippa, G.; Xie, Y.; Gu, X. phenofit: An R package for extracting vegetation phenology from time series remote sensing. *Methods Ecol. Evol.* **2022**, *13*, 1508–1527. [CrossRef]
37. Li, Y.; Zhang, W.; Schwalm, C.R.; Gentine, P.; Smith, W.K.; Ciais, P.; Kimball, J.S.; Gazol, A.; Kannenberg, S.A.; Chen, A.; et al. Widespread spring phenology effects on drought recovery of Northern Hemisphere ecosystems. *Nat. Clim. Change* **2023**, *13*, 182–188. [CrossRef]
38. Savitzky, A.; Golay, M.J.E. Smoothing and differentiation of data by simplified least squares procedures. *Anal. Chem.* **1964**, *36*, 1627–1639. [CrossRef]
39. Sisheber, B.; Marshall, M.; Mengistu, D.; Nelson, A. Tracking crop phenology in a highly dynamic landscape with knowledge-based Landsat–MODIS data fusion. *Int. J. Appl. Earth Obs. Geoinf.* **2022**, *106*, 102670. [CrossRef]
40. Guo, J.; Yang, X.; Niu, J.; Jin, Y.; Xu, B.; Shen, G.; Zhang, W.; Zhao, F.; Zhang, Y. Remote sensing monitoring of green-up dates in the Xilingol grasslands of northern China and their correlations with meteorological factors. *Int. J. Remote Sens.* **2018**, *40*, 2190–2211. [CrossRef]
41. Jonsson, P.; Eklundh, L. Seasonality extraction by function fitting to time-series of satellite sensor data. *IEEE Trans. Geosci. Remote Sens.* **2022**, *40*, 1824–1832. [CrossRef]
42. Hou, D.; Al-Tabbaa, A.; Chen, H.; Mamic, I. Factor analysis and structural equation modelling of sustainable behaviour in contaminated land remediation. *J. Clean. Prod.* **2014**, *84*, 439–449. [CrossRef]
43. Lu, J.; Qin, T.; Yan, D.; Lv, X.; Yuan, Z.; Wen, J.; Xu, S.; Yang, Y.; Feng, J.; Li, W. Response of vegetation to drought in the source region of the Yangtze and Yellow Rivers based on causal analysis. *Remote Sens.* **2024**, *16*, 630. [CrossRef]
44. Cheung, M.W. Comparison of approaches to constructing confidence intervals for mediating effects using structural equation models. *Struct. Equ. Model. A Multidiscip. J.* **2007**, *14*, 227–246. [CrossRef]
45. Chen, A.; Yang, X.; Xu, B.; Jin, Y.; Guo, J.; Xing, X.; Yang, D.; Wang, P.; Zhu, L. Monitoring the spatiotemporal dynamics of aeolian desertification using Google Earth Engine. *Remote Sens.* **2021**, *13*, 1730. [CrossRef]
46. Lin, M.; Hou, L.; Qi, Z.; Wan, L. Impacts of climate change and human activities on vegetation NDVI in China's Mu Us Sandy Land during 2000–2019. *Ecol. Indic.* **2022**, *142*, 109164. [CrossRef]
47. Zhang, J.; Wang, J.; Liu, L.; Liu, H.; Liu, Y.; Li, M. On potential salient climatic factors tied to late-summer compound drought and heatwaves around Horqin sandy land, Northeast China. *Theor. Appl. Climatol.* **2024**, *155*, 6829–6842. [CrossRef]
48. Liu, S.; Zhao, H.; Dong, S.; Su, X.; Liu, Q.; Zhang, X. Landscape dynamics along a river corridor in alpine desert region and its driving factor analysis: A case study in Altun National Nature Reserve. *Chin. J. Ecol.* **2014**, *33*, 1647–1654. Available online: https://www.researchgate.net/publication/288442867_Landscape_dynamics_along_a_river_corridor_in_alpine_desert_region_and_its_driving_factor_analysis_A_case_study_in_Altun_National_Nature_Reserve (accessed on 27 July 2024).
49. Zhang, Y.; Lu, Y.; Sun, G.; Li, L.; Zhang, Z.; Zhou, X. Dynamic Changes in Vegetation Ecological Quality in the Tarim Basin and Its Response to Extreme Climate during 2000–2022. *Forests* **2024**, *15*, 505. [CrossRef]
50. Feng, J.; Yan, D.; Li, C.; Gao, Y.; Liu, J. Regional Frequency Analysis of Extreme Precipitation after Drought Events in the Heihe River Basin, Northwest China. *J. Hydrol. Eng.* **2014**, *19*, 1101–1112. [CrossRef]
51. Ma, S.; Ren, J.; Wu, C.; He, Q. Extreme precipitation events trigger abrupt vegetation succession in emerging coastal wetlands. *Catena* **2024**, *241*, 108066. [CrossRef]
52. Tuo, M.; Xu, G.; Zhang, T.; Guo, J.; Zhang, M.; Gu, F.; Wang, B.; Yi, J. Contribution of climatic factors and human activities to vegetation changes in arid grassland. *Sustainability* **2024**, *16*, 794. [CrossRef]
53. Dong, T.; Liu, J.; Shi, M.; He, P.; Li, P.; Liu, D. Seasonal scale climatic factors on Grassland phenology in Arid and Semi-Arid Zones. *Land* **2024**, *13*, 653. [CrossRef]
54. Ying, H.; Zhang, H.; Zhao, J.; Shan, Y.; Zhang, Z.; Guo, X.; Rihan, W.; Deng, G. Effects of spring and summer extreme climate events on the autumn phenology of different vegetation types of Inner Mongolia, China, from 1982 to 2015. *Ecol. Indic.* **2019**, *111*, 105974. [CrossRef]
55. He, Z.; Du, J.; Chen, L.; Zhu, X.; Lin, P.; Zhao, M.; Fang, S. Impacts of recent climate extremes on spring phenology in arid-mountain ecosystems in China. *Agric. For. Meteorol.* **2018**, *260–261*, 31–40. [CrossRef]
56. Zhang, S.; Zhang, J.; Liang, S.; Liu, S.; Zhou, Y. A perception of the nexus "resistance, recovery, resilience" of vegetations responded to extreme precipitation pulses in arid and semi-arid regions: A case study of the Qilian Mountains Nature Reserve, China. *Sci. Total Environ.* **2022**, *843*, 157105. [CrossRef]
57. Shen, Y.; Shen, Y.; Guo, Y.; Zhang, Y.; Pei, H.; Brenning, A. Review of historical and projected future climatic and hydrological changes in mountainous semiarid Xinjiang (northwestern China), central Asia. *Catena* **2020**, *187*, 104343. [CrossRef]
58. Xu, B.; Arain, M.A.; Black, T.A.; Law, B.E.; Pastorello, G.Z.; Chu, H. Seasonal variability of forest sensitivity to heat and drought stresses: A synthesis based on carbon fluxes from North American forest ecosystems. *Glob. Change Biol.* **2019**, *26*, 901–918. [CrossRef]
59. Shao, H.; Zhang, Y.; Gu, F.; Shi, C.; Miao, N.; Liu, S. Impacts of climate extremes on ecosystem metrics in southwest China. *Sci. Total Environ.* **2021**, *776*, 145979. [CrossRef]